

# Capsaicin Attenuates LPS-Induced Acute Lung Injury by Inhibiting Inflammation and Autophagy Through Regulation of the TRPV1/AKT Pathway

Qin Hu <sup>1,2</sup>, Haoran Liu <sup>1,2</sup>, Ruiyu Wang<sup>3</sup>, Li Yao<sup>3</sup>, Shikun Chen <sup>4</sup>, Yang Wang<sup>3</sup>, Chuanzhu Lv<sup>2,3,5</sup>

<sup>1</sup>Emergency and Trauma College, Hainan Medical University, Haikou, People's Republic of China; <sup>2</sup>Key Laboratory of Emergency and Trauma of Ministry of Education, Hainan Medical University, Haikou, People's Republic of China; <sup>3</sup>Emergency Medicine Center, Sichuan Provincial People's Hospital, University of Electronic Science and Technology of China, Chengdu, People's Republic of China; <sup>4</sup>Department of Anesthesiology, the Second Affiliated Hospital of Chongqing Medical University, Chongqing, People's Republic of China; <sup>5</sup>Research Unit of Island Emergency Medicine, Chinese Academy of Medical Sciences (No. 2019RU013), Hainan Medical University, Haikou, People's Republic of China

Correspondence: Yang Wang, Emergency Medicine Center, Sichuan Provincial People's Hospital, University of Electronic Science and Technology of China, Chengdu, People's Republic of China, Tel +86-15086867864, Email young0416@163.com; Chuanzhu Lv, Key Laboratory of Emergency and Trauma of Ministry of Education, Hainan Medical University, Research Unit of Island Emergency Medicine, Chinese Academy of Medical Sciences (No. 2019RU013), Hainan Medical University, Haikou, People's Republic of China, Tel +86- 19113953671, Email lvchuanzhu677@126.com

**Purpose:** Acute lung injury (ALI) is a severe pulmonary disease characterized by damage to the alveoli and pulmonary blood vessels, leading to severe impairment of lung function. Studies on the effect of capsaicin (8-methyl-N-geranyl-6-nonamide, CAP) on lipopolysaccharide (LPS)-induced ALI in bronchial epithelial cells transformed with Ad12-SV40 2B (BEAS-2B) are still limited. This study aimed to investigate the effect and specific mechanism by which CAP improves LPS-induced ALI.

**Methods:** The present study investigated the effect of CAP and the potential underlying mechanisms in LPS-induced ALI in vitro and vivo via RNA sequencing, Western blotting (WB), quantitative real-time reverse transcription PCR (qRT-PCR), enzyme-linked immunosorbent assay (ELISA), and transmission electron microscopy (TEM). The TRPV1 inhibitor AMG9810 and the AKT agonist SC79 were used to confirm the protective effect of the TRPV1/AKT axis against ALI. The autophagy agonist rapamycin (Rapa) and the autophagy inhibitors 3-methyladenine (3-MA) and bafilomycin A1 (Baf-A1) were used to clarify the characteristics of LPS-induced autophagy.

**Results:** Our findings demonstrated that CAP effectively suppressed inflammation and autophagy in LPS-induced ALI, both in vivo and in vitro. This mechanism involves regulation by the TRPV1/AKT signaling pathway. By activating TRPV1, CAP reduces the expression of P-AKT, thereby exerting its anti-inflammatory and inhibitory effects on pro-death autophagy. Furthermore, prior administration of CAP provided substantial protection to mice against ALI induced by LPS, reduced the lung wet/dry ratio, decreased proinflammatory cytokine expression, and downregulated LC3 expression.

**Conclusion:** Taken together, our results indicate that CAP protects against LPS-induced ALI by inhibiting inflammatory responses and autophagic death through the TRPV1/AKT signaling pathway, presenting a novel strategy for ALI therapy.

**Keywords:** capsaicin, acute lung injury, Inflammation, autophagy, TRPV1, AKT

## Introduction

Acute lung injury (ALI) is a collection of clinical syndromes resulting from injury to alveolar epithelial cells and capillary endothelial cells, manifesting as widespread damage to the alveolar parenchyma and intractable hypoxemia. The hallmark features of ALI include diffuse alveolar injury, formation of hyaline membranes, and thickening of the interstitium. In severe cases, ALI can progress to pulmonary fibrosis and ultimately acute respiratory distress syndrome (ARDS).<sup>1,2</sup> The pathogenesis of ALI is characterized by the occurrence of functional cell apoptosis, systemic inflammation, and disruption of lung immune homeostasis. These processes collectively contribute to the development of life-threatening organ failure.<sup>3</sup> ALI is a severe inflammatory syndrome that poses a significant threat to life, resulting in high

mortality and morbidity rates. However, ALI patients rarely return to normal after treatment, resulting in physical and psychological suffering. Therefore, the development of effective drugs to alleviate inflammatory responses and further improve long-term prognosis in patients with ALI has become an urgent and important issue.

The stimulation of lipopolysaccharide (LPS) triggers the activation of neutrophils and macrophages, prompting them to release several proinflammatory cytokines, such as tumor necrosis factor- $\alpha$  (TNF- $\alpha$ ), interleukin-6 (IL-6), and interleukin-1 $\beta$  (IL-1 $\beta$ ).<sup>4</sup> LPS-induced bronchial epithelial cells transformed with Ad12-SV40 2B (BEAS-2B) have been extensively utilized as a clinically relevant model of ALI due to their ability to accurately simulate pathological events such as inflammation and histological alterations.<sup>5,6</sup>

In recent years, proprietary Chinese medicines have become essential players in the clinical treatment of diseases. For example, studies have shown that cryptotanshinone<sup>7</sup> and scutellarein<sup>8</sup> can alleviate chronic obstructive pulmonary disease, and sodium houttuynia<sup>6</sup> has a protective effect against chronic airway inflammation. Capsaicin (8-methyl-N-geranyl-6-nonamide, CAP) is a naturally occurring substance extracted from *Capsicum annuum* in the Solanaceae family, that has exerted multiple pharmacological effects and therapeutic effects on various diseases, including cancer,<sup>9</sup> diabetic cardiovascular disease<sup>10</sup> and pain.<sup>11</sup> In addition, CAP has also exerted significant therapeutic effects on acute liver injury,<sup>12</sup> colitis,<sup>13</sup> and LPS-induced inflammation in macrophages.<sup>14</sup> Currently, there are various ointments containing CAP that can be topically applied to alleviate pain, migraines, headaches, psoriasis, and infections caused by the herpes simplex virus.<sup>15,16</sup> Additionally, CAP has shown promising therapeutic potential in mitigating symptoms related to dyspepsia, decreased appetite, excessive gas, arterial plaque buildup, cardiovascular disorders, and muscle tension.<sup>17</sup> According to recent studies, CAP has been found to relieve LPS-induced ALI in vivo through the HMGB1/NF- $\kappa$ B and PI3K/AKT/mTOR pathways.<sup>18</sup> Furthermore, several research studies have suggested that transient receptor potential vanilloid type 1 (TRPV1), which is stimulated by CAP, may have various physiological impacts.<sup>19</sup> However, the role of TRPV1 activation by CAP in the treatment of LPS-induced ALI in BEAS-2B cells remains elusive.

Autophagy, a crucial biological process involved in the degradation and removal of detrimental proteins and organelles within cells via autophagosome formation,<sup>20</sup> plays a pivotal role in maintaining cellular viability. Autophagy is constitutively present at basal levels under physiological conditions and plays a pivotal role in maintaining intracellular homeostasis. Nevertheless, the occurrence of irregular autophagy has been associated with the emergence of diverse lung ailments, such as fibrotic lung disease,<sup>21</sup> obstructive pulmonary disease,<sup>22</sup> and pulmonary injury.<sup>23,24</sup> Studies have shown that inhibiting LPS-induced excessive autophagy in alveolar epithelial cells can mitigate inflammatory injury.<sup>25,26</sup> Moreover, excessive autophagy activation has been implicated in the development of ALI,<sup>27–30</sup> and the effective inhibition of autophagy is a potential therapeutic approach. Thus, modulating autophagy from inducing death to supporting survival could prove effective in the treatment of LPS-induced ALI. However, whether the anti-inflammatory effect of CAP against LPS-induced ALI in BEAS-2B cells is associated with autophagy remains poorly understood, necessitating further investigation.

Therefore, this study performed RNA sequencing, enzyme-linked immunosorbent assay (ELISA), quantitative real-time reverse transcription PCR (qRT-PCR), and Western blotting (WB) to explore whether LPS-induced inflammation and autophagy can be reversed in vitro and in vivo, as well as the characteristics of autophagy in response to CAP.

## Materials and Methods

### Reagents and Chemicals

BEAS-2B cells (Cat. No. CRL9609) were obtained from the American Type Culture Collection (ATCC) located in Manassas, VA, USA. Gibco (Grand Island, NY, USA) provided Dulbecco's modified Eagle's medium (DMEM), fetal bovine serum, phosphate-buffered saline (PBS), trypsin, and dual-antibiotics. Beyotime Biotech (Shanghai, China) provided the CCK-8 cell viability and cytotoxicity test kit, RIPA lysis buffer, phenylmethanesulfonyl fluoride (PMSF), the bicinchoninic acid (BCA) protein assay kit, and bovine serum albumin (BSA). The CellTiter 96 AQueous One Solution Cell Proliferation Assay (MTS) Kit is provided by Promega (Beijing, China). CAP was sourced from MedChemExpress (Shanghai, China), while LPS was obtained from Sigma-Aldrich (St. Louis, MO, USA). Rapamycin (Rapa) (S1039), 3-methyladenine (3-MA) (S2767), bafilomycin A1 (Baf-A1) (S1413), AMG9810 (S6934), and SC79 (S7863) were acquired from Selleck (Houston, USA). Anti-

TNF- $\alpha$  (GB11188) antibodies were obtained from Servicebio (Wuhan, China). Anti-p-AKT (cat. 4060S), anti-AKT (cat. 9272S), anti-p-p65 (cat. 3033S), anti-p65 (cat. 8242S), anti-LC3 A/B (cat. 12741S), and anti-P62/SQSTM1 (cat. 88588S) antibodies were obtained from Cell Signaling Technology (Boston, MA, USA). Anti-TRPV1 (Cat No: 66983-1-Ig) was acquired from Proteintech (Wuhan, China). Anti-p-PI3K (AF3242) was obtained from Affinity (Jiangsu, China). Alexa Fluor 488 (HA1121)- and Alexa Fluor 594 (HA1126)- conjugated secondary antibodies, anti-PI3K (ET1610-36) and anti-GAPDH (ET1601-4) were purchased from HuaBio (China).

## RNA Sequencing

After RNA extraction (Invitrogen TRIzol), purification (Thermo Scientific NanoDrop 2000; Thermo Scientific, Waltham, Massachusetts, USA), and library preparation (NEBNext Ultra II RNA Library Prep Kit for Illumina), the samples were subjected to next-generation sequencing (NGS) on the Illumina sequencing platform, and RNA-seq was performed using PANOMIX. DESeq software (version 1.20.0) was utilized for conducting differential expression analysis between two groups. For Gene Ontology (GO) enrichment analysis, topGO was employed. The hypergeometric distribution method was used to calculate P values, with significance defined as a P value < 0.05. Kyoto Encyclopedia of Genes and Genomes (KEGG) pathway enrichment analysis was performed using clusterProfiler software (version 3.4.4), with a focus on significantly enriched pathways with P values < 0.05. Differential splicing events were analyzed using rMATS software (version 3.2.5), with a focus on five major types of alternative splicing events: SE, RI, MXE, A5SS, and A3SS.

## Cell Culture and Treatment

To cultivate cells, DMEM basal medium was supplemented with 10% fetal bovine serum and 1% penicillin–streptomycin. The cells were grown in a moist incubator at a consistent temperature of 37°C and 5% CO<sub>2</sub>. For the treatments, BEAS-2B cells were subjected to different conditions. Initially, the cells were categorized into four groups: Vehicle, CAP, LPS, and CAP+LPS. The cells were cultured in the presence or absence of CAP (100  $\mu$ mol/l) for 1 h. Subsequently, the cells were further treated with LPS (10  $\mu$ g/mL) for 6 h.<sup>6,31,32</sup> In another set of experiments, the cells were pretreated with AMG9810 (10  $\mu$ mol/l)<sup>33</sup> or SC79 (10  $\mu$ mol/l)<sup>34</sup> for 2 h before CAP treatment. Subsequently, these cells were exposed to LPS for 6 h before further experiments were conducted.

## Cell Viability Assay

The BEAS-2B cells were planted in a 96-well plate at a density of  $5 \times 10^4$ /mL, 100  $\mu$ L per well. The cells were treated with CAP at concentrations of 0, 50, 100, 200, 400, 600, or 800  $\mu$ mol/l for 12 or 24 h, and then the IC<sub>50</sub> of CAP was determined in BEAS-2B cells. The results of the IC<sub>50</sub> assay are shown in [Supplementary Material Figure S1](#). In a 96-well plate, BEAS-2B cells were seeded at a concentration of  $3 \times 10^4$  cells/mL. Different concentrations of CAP (0, 50, 100, 150  $\mu$ mol/l) were added to the wells, and the cells were incubated for 12 h or 24 h. Subsequently, 10  $\mu$ L of CCK-8 detection reagent was added to each well, and the cells were incubated for 1 h. A microplate reader was utilized to measure the absorbance at 450 nm, enabling the assessment of cell viability. To evaluate the autophagic properties following 6 h of LPS stimulation, different groups were established. The treatments included the Vehicle, LPS, LPS+Rapa (100 nmol/l),<sup>35,36</sup> LPS+3-MA (5 mmol/l),<sup>37,38</sup> and LPS+Baf-A1 (100 nmol/l)<sup>39</sup> groups, which were treated with the respective activators or inhibitors for 2 h prior to LPS stimulation. Subsequently, the groups were subjected to 6 h of LPS stimulation. Then, the original culture medium was aspirated, and 10  $\mu$ L of the CCK-8 detection reagent was added to each well. After incubating for 1 h, the absorbance at 450 nm was measured using a microplate reader to determine cell viability. The cell viability was calculated using Equation 1.

$$\text{Cell viability (\%)} = \frac{(\text{OD}_{\text{experiment}} - \text{OD}_{\text{blank}})}{(\text{OD}_{\text{control}} - \text{OD}_{\text{blank}})} \times 100\% \quad (1)$$

## Quantifying Cell Proliferation Using the MTS Assay

As shown in the CCK-8 procedure, Beas-2B cells were seeded into a 96-well plate according to the groups, with 3 replicate wells for each group, along with three wells of cell-free and untreated blank controls. After the corresponding treatment time, the culture medium was removed, and 20  $\mu$ L of MTS reagent was added to each well. The plate was then

incubated at 37°C with 5% CO<sub>2</sub> for 1 to 4 h, after which the absorbance at 490 nm was measured. The cell viability was calculated using Equation 1. The results of the MTS cell viability assay are shown in [Supplementary Material Figure S2](#).

## ELISA

TNF- $\alpha$ , IL-6, and IL-1 $\beta$  levels were quantified in cell supernatants and mouse serum using commercially available ELISA kits (Solarbio, Beijing China) according to the manufacturer's instructions.

## WB

Following the administration of various treatment regimens for the specified durations, the cells were subjected to lysis using RIPA lysis buffer supplemented with PMSF and phosphatase inhibitors to extract the entirety of intracellular proteins. The protein concentration in the lysates was determined using a BCA protein assay kit. Subsequently, the protein samples were separated on 8–12% gels by SDS–PAGE and transferred onto polyvinylidene fluoride (PVDF) membranes (Millipore, USA) using a semidry transfer apparatus (Bio-Rad, 690BR035335). Subsequently, the membranes were blocked with 5% skim milk or 5% BSA for 1 h at room temperature, followed by overnight incubation at 4°C with the appropriate primary antibodies (1:1000). After washing the membranes with Tris-buffered saline containing Tween-20 (TBST), they were subsequently incubated with secondary antibodies for 1 h at 37°C. Following another round of washing, the reactive protein bands were visualized using an enhanced chemiluminescence (ECL) detection system and captured on film. The intensity of the protein bands was quantified using ImageJ software, and GAPDH served as a loading control.

## qRT–PCR

Total cellular RNA and total lung tissue RNA were extracted by a TransZol (Trans Gene Biotech) kit. qRT–PCR was performed with an Ambion 7500 Real-Time PCR System (Thermo Fisher) using the TransZol kit. The samples were amplified in triplicate within a single run. GAPDH was employed as an internal reference, and the relative expression levels of genes were determined using the  $2^{-\Delta\Delta C_t}$  method. The results are presented as the ratio to the internal reference.

The cellular primer sequences were as follows: human GAPDH, 5'-AGAAGGCTGGGGCTCATTTG-3' and 5'-AGGGGCCATCCACAGTCTTC-3'; human TNF- $\alpha$ , 5'-CGAGTCTGGGCAGGTCTA-3' and 5'-GTGGTGGTCTTGT TGCTTAA-3'; human IL-6, 5'-GGAGACTTGCCTGGTGAA-3' and 5'-GCATTTGTGGTTGGGTCA-3'; and human IL-1 $\beta$ , 5'-ACAGTGGCAATGAGGATG-3' and 5'-TGTAGTGGTGGTCGGAGA-3'.

The mouse tissue primer sequences were as follows: mouse GAPDH, 5'-GTGAAGGTCCGGTGTGAACGGATT -3' and 5'-CTCGCTCCTGGAAGATGGTGATG-3'; mouse TNF- $\alpha$ , 5'-AGCCAGGAGGGAGAACAGAAACT-3' and 5'-GCCACAAGCAGGAATGAGAAGAGG-3'; mouse IL-6, 5'-TGTCTGTAGCTCATTCTGCTCTGG-3' and 5'-GAAGGCAACTGGATGGAAGTCTCT-3'; and mouse IL-1 $\beta$ , 5'-GAAATGCCACCTTTTGACAGTG-3' and 5'-TGGATGCTCTCATCAGGACAG-3'.

## Transmission Electron Microscopy (TEM)

BEAS-2B cells were subjected to various treatments, including CAP and LPS exposure. Subsequently, the cells were gently rinsed with 1 $\times$  phosphate-buffered saline (PBS) at a pH of 7.3 and room temperature. Afterward, the cells were collected, preserved in a solution comprising 2.5% glutaraldehyde and 1% osmic acid, dehydrated using escalating amounts of ethanol and acetone, embedded, cut into sections, and finally stained with a blend of 3% uranyl acetate and lead citrate. Finally, the cells were examined using a transmission electron microscope (Hitachi, HT7800/HT7700).

## Immunofluorescence Analysis

After being washed three times with PBS, the cells were treated with methanol for 10 min to fix and permeabilize them and then blocked with a blocking buffer for another 10 min. Primary antibodies against LC3 (1:50–200) and P62 (1:200–800) were added to the cells and incubated overnight at 4°C. On the following day, the cells underwent three rounds of washing using PBS. Subsequently, they were exposed to Alexa Fluor 488 (1:500)- or Alexa Fluor 594 (1:500)- conjugated secondary antibodies at room temperature for 1 h. Following the removal of the secondary antibodies, the cells were washed three more times and then

counterstained with DAPI for 15 min to stain the nuclei. Finally, the cells were captured using a confocal microscope from Carl Zeiss in Jena, Germany. All subsequent procedures starting from secondary antibody incubation were carried out in the dark.

## Animal Experiments

All animal protocols were reviewed and approved by the Animal Care and Use Committee of Sichuan Provincial People's Hospital. Male BALB/c mice (6–8 weeks old) were purchased from Beijing Vital River Laboratory Animal Technology Co., Ltd. (License No. SCXK(京)2021–0006). Following a period of 1–2 weeks in the specified conditions, the mice were divided into four groups (each group consisting of six mice weighing approximately  $21 \pm 1$  g): Vehicle, CAP, LPS, and CAP+LPS. The CAP and CAP+LPS groups were intraperitoneally injected with CAP (8 mg/kg)<sup>40</sup> daily for 5 days before the experiment. The Vehicle group received daily intraperitoneal injections of an equivalent volume of saline solution. On the fifth day, the LPS and CAP+LPS groups were intratracheally injected with LPS (5 mg/kg).<sup>41,42</sup> Twelve hours later, the mice were euthanized by intraperitoneal injection of pentobarbital sodium (5%, 50 mg/kg). Lung tissue, serum, and bronchoalveolar lavage fluid (BALF) were collected for further experimentation.

## Collection of Mouse Serum

Following anesthesia, the mice were dissected, and blood samples were extracted from the heart. To facilitate clotting, the collected blood was left undisturbed at room temperature for a duration of 30–60 min. After the clotting process, the blood samples were subjected to centrifugation at 14,000 rpm for 20 min at room temperature. The resulting supernatant, consisting of serum, was meticulously transferred to a clean centrifuge tube. To maintain stability, serum samples were then stored at  $-80^{\circ}\text{C}$  for subsequent use.

## Collection of BALF

After lavaging the lungs with 1 mL of PBS three times, BALF was collected. The collected BALF was then subjected to centrifugation at  $1000 \times g$  for 10 min at  $4^{\circ}\text{C}$ . The resulting supernatant was frozen at  $-80^{\circ}\text{C}$  for later analysis. The total protein concentrations in the BALF were measured using a BCA protein assay kit.

## Hematoxylin-Eosin (HE) Staining

Each sample underwent fixation using a 10% (v/v) neutral formalin solution, followed by embedding in paraffin and sectioning into 4  $\mu\text{m}$  thick slices. These slices were then stained using an HE staining kit (Servicebio, G1003) according to the provided instructions. The control group, which utilized  $1 \times$  PBS (pH=7.3, at room temperature), was used as a reference. A semiquantitative system was employed to calculate the tissue pathological score and assess the extent of congestion, hemorrhage, alveolar wall edema, and inflammatory cell infiltration in each group. The severity of lung injury was graded on a scale ranging from 0 to 4.5, where 0 represents a normal condition, 0.5 indicates mild or very small abnormalities, 1 signifies mild or small abnormalities, 2 represents moderate or more abnormalities, 3 indicates severe or many abnormalities, and 4 represents extremely severe or extremely large abnormalities.<sup>43</sup>

## Immunohistochemistry (IHC)

Pulmonary sample paraffin sections were first heated in an oven, followed by xylene-based deparaffinization and rehydration via a series of ethanol solutions. These sections were then subjected to microwave treatment in sodium citrate buffer. Once cooled to room temperature, these slides were exposed to 3% fresh hydrogen peroxide. Afterward, the sections were blocked with 3% bovine serum albumin (BSA) at ambient temperature, followed by an overnight incubation at  $4^{\circ}\text{C}$  with primary antibodies specific to TNF- $\alpha$ , P-AKT, LC3, and TRPV1. After incubation, the slides were thoroughly rinsed with PBS and incubated with secondary and tertiary antibodies for 20 min at  $37^{\circ}\text{C}$ . Subsequently, sections were exposed to DAB substrate and counterstained with hematoxylin in a light-protected environment. Following a dehydration and drying sequence, the sections were mounted using neutral gum. Ultimately, slide evaluation was performed under a microscope.

## Determination of the Lung Wet/Dry Weight Ratio

The right upper lobe of the lung was meticulously harvested and washed using PBS. Subsequently, the tissue was gently dried on blotting paper, and the initial wet weight was recorded. The lung tissue was subsequently placed in a drying oven and subjected to a drying period of 72 h at 60°C. Following the completion of the drying procedure, the tissue was weighed once more, indicating the final dry weight. The wet/dry weight ratio was calculated by dividing the initial wet weight by the final dry weight.

## Statistical Analysis

The data are presented as the mean  $\pm$  standard deviation (SD). Graphs were created, and statistical analyses were conducted using GraphPad Prism 8 software (San Diego, CA). For comparisons between two groups, t tests were employed, while one-way analysis of variance (ANOVA) was utilized for comparisons between multiple groups. Statistical significance was defined as a p value below 0.05.

## Results

### CAP Exerts Anti-Inflammatory Effects on BEAS-2B Cells

The two-dimensional chemical structure of CAP is shown in [Figure 1a](#). We measured the IC<sub>50</sub> of CAP in BEAS-2B cells using a CCK-8 assay. The results showed that the IC<sub>50</sub> was 445.9  $\mu\text{mol/l}$  when the cells were treated with CAP for 12 hours ([Figure S1a](#)) and 350.2  $\mu\text{mol/l}$  when the cells were treated for 24 hours ([Figure S1b](#)). Then, we determined the safe concentration of CAP for the subsequent treatment of BEAS-2B cells. The CCK-8 assay was used to determine cell viability, as shown in [Figure 1b](#). Notably, there was no significant change in survival when the cells were treated with 50, 100, or 150  $\mu\text{mol/l}$  CAP for 12 h or 24 h. The results showed that less than 150  $\mu\text{mol/l}$  CAP did not damage cells. Therefore, we chose 100  $\mu\text{mol/l}$  CAP as the therapeutic concentration. Subsequently, we induced inflammation with 10  $\mu\text{g/mL}$  LPS for 6 h and pretreated the cells with the indicated concentration of CAP for 1 h. Inflammatory mediators, including TNF- $\alpha$ , IL-1 $\beta$ , and IL-6, play crucial roles in the development of LPS-induced ALI. Therefore, we validated the effects of CAP on these three factors using qRT-PCR. The results ([Figure 1c](#)) showed that 100  $\mu\text{mol/l}$  CAP significantly inhibited the LPS-induced upregulation of the mRNA expression of the inflammatory genes TNF- $\alpha$ , IL-6, and IL-1 $\beta$ .

### CAP Pretreatment Inhibits LPS-Induced Inflammatory Cytokine Release and Activation of PI3K/AKT and NF- $\kappa$ B

To further investigate the inhibitory effect of CAP on inflammation, we used ELISA to measure the expression levels of proinflammatory cytokines (TNF- $\alpha$ , IL-1 $\beta$ , and IL-6) in the different groups, and changes in cell viability were assessed by CCK-8 and MTS assays. The results showed that CAP pretreatment reduced the levels of these proinflammatory cytokines ([Figure 2a](#)). Additionally, CCK8 ([Figure 2b](#)) and MTS ([Figure S2a](#)) assay results shows that LPS stimulation significantly reduced cell viability. However, this decrease in cell viability was partially reversed by CAP pretreatment. To further clarify the mechanism by which CAP ameliorates ALI, we performed RNA sequencing of the treated cells on the Illumina platform to analyze the pathway targets by which CAP inhibits LPS-induced inflammatory cytokine release. The RNA sequencing results shown in the figures were all obtained from comparisons between the CAP+LPS group and the LPS group. The volcano map ([Figure 2c](#)) shows that 30 genes were upregulated and 46 were downregulated. GO ([Figure 2d](#)) and KEGG ([Figure 2e](#)) enrichment analyses were used to identify the pathways associated with inflammation. The results indicated that inhibiting PI3K/AKT and NF- $\kappa$ B activation may be one of the mechanisms by which CAP can be used to treat ALI. Therefore, we performed WB ([Figure 2f](#)) to examine the activation of PI3K, AKT, and p65. The results ([Figure 2g](#)) showed that LPS stimulation significantly increased the expression of the phosphorylated forms of PI3K, AKT, and p65. However, pretreatment with CAP partially reversed the changes in these proteins. Taken together, these findings indicate that CAP pretreatment can effectively mitigate LPS-induced cellular inflammation by inhibiting activation of the PI3K/AKT and NF- $\kappa$ B signaling pathways. Furthermore, CAP alone did not induce any significant changes in the expression of proinflammatory cytokines.

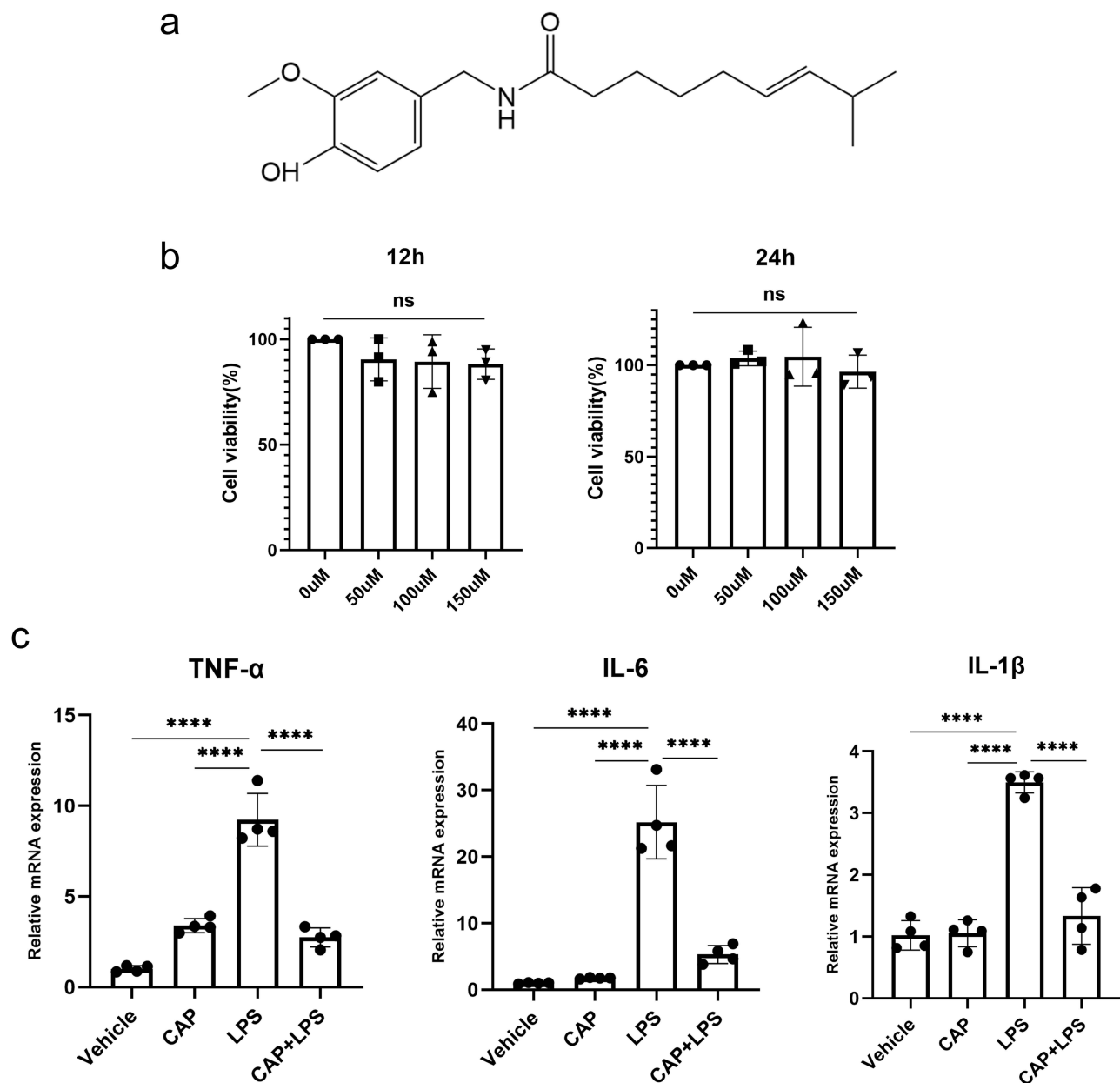


**Figure 1** The optimal concentration of CAP for treating BEAS-2B cells was 100  $\mu\text{M}$ . (a) The chemical formula of CAP (b) BEAS-2B cells were treated with 0, 50, 100, and 150  $\mu\text{M}$  CAP. Cell viability for 12 h or 24 h was measured using the CCK-8 assay. (c) qRT-PCR was used to determine the gene expression levels of TNF- $\alpha$ , IL-6, and IL-1 $\beta$  in LPS-stimulated BEAS-2B cells treated with 100  $\mu\text{M}$  CAP. (n=3~4) \*\*\*\*P < 0.0001.

## CAP Reduces LPS-Induced Autophagy

To further understand whether CAP ameliorates ALI by inhibiting autophagy, we compared autophagy in cells in the Vehicle, CAP, LPS, and CAP+LPS groups and performed WB and immunofluorescence analysis of LC3 and P62, which are indicators of autophagy. Consistent with previous studies,<sup>44,45</sup> we observed that the protein levels of LC3 (Figure 3a and b) were significantly increased in the LPS group compared to the Vehicle and CAP groups. Conversely, the expression of P62 was decreased in the LPS group. In the CAP+LPS group, the change in expression was reversed. TEM can be used to examine the morphology and number of autolysosomes and intracellular autophagosomes and observe autophagy status, making it the gold standard for examining autophagy. TEM (Figure 3c) revealed an increased number of autophagosomes in the LPS group, while the number of autophagosomes in the CAP+LPS group was decreased. The order of autophagosome numbers in the four groups was as follows: LPS > CAP+LPS > CAP > Vehicle. In addition, TEM quantitative analysis (Figure 3d) also showed that the number of autophagosomes and autolysosomes was significantly lower in the CAP+LPS group than in the LPS group.

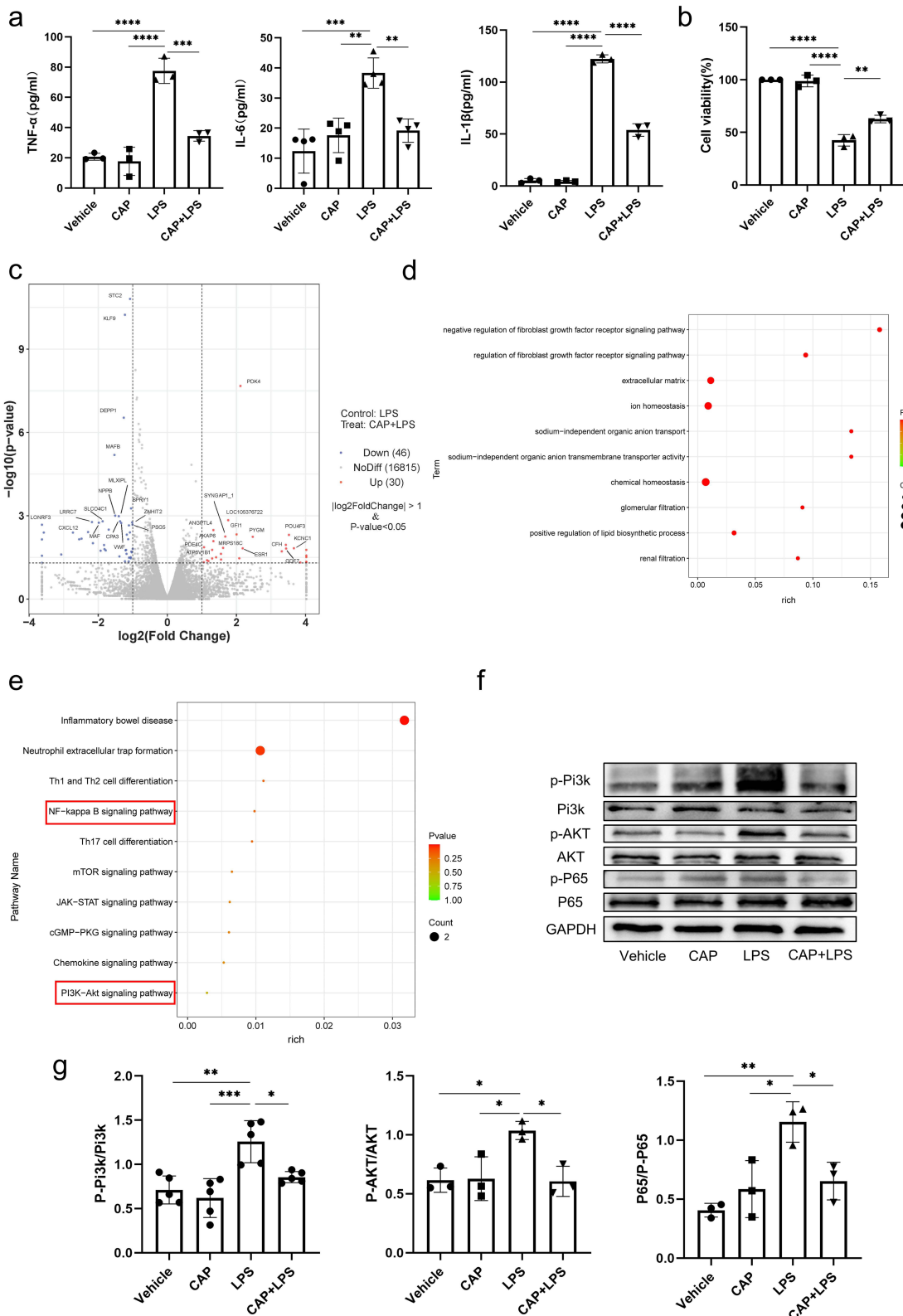


**Figure 2** CAP alleviates inflammation in LPS-stimulated BEAS-2B cells. (a) ELISA kits were used to measure levels of TNF- $\alpha$ , IL-6, and IL-1 $\beta$ . (b) Cell viability was assessed using the CCK-8 assay. (c) Volcano plot. (d) GO enrichment analysis of CAP pretreated BEAS-2B cells after LPS stimulation (top 10 inflammation-related pathways). (e) KEGG enrichment analysis of CAP pretreated BEAS-2B cells after LPS stimulation (top 10 inflammation-related pathways). (f) The expression levels of critical proteins involved in the PI3K/AKT and NF- $\kappa$ B signaling pathways were measured by WB. (g) Statistical analyses of p-PI3K, p-AKT, and p-p65 in BEAS-2B cells. (n=3-5) \*P < 0.05, \*\*P < 0.01, \*\*\*P < 0.001, \*\*\*\*P < 0.0001.

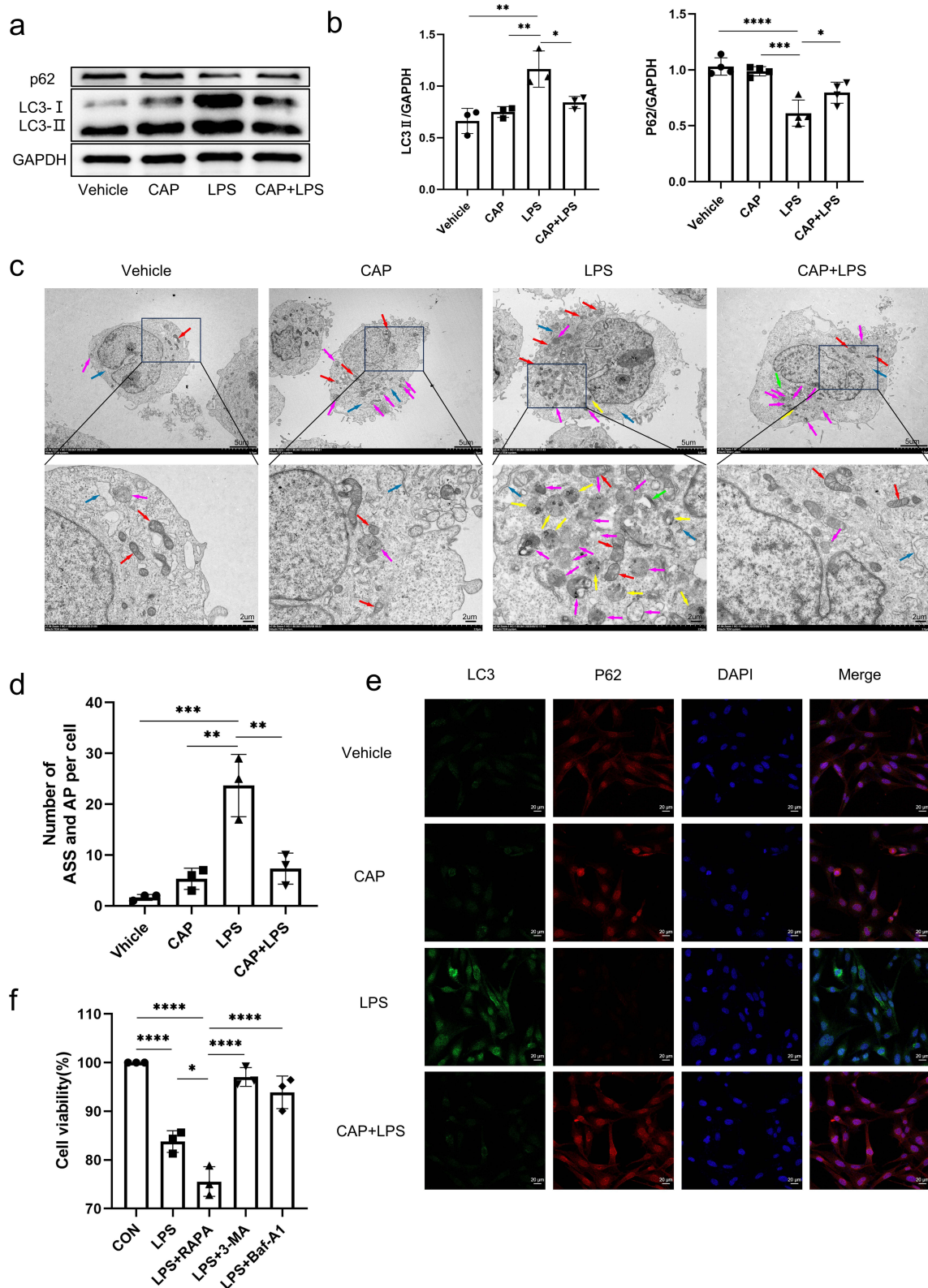


**Figure 3** CAP alleviates autophagy in LPS-stimulated BEAS-2B cells. (a) WB was used to detect the expression of LC3II and P62. (b) Statistical analyses of LC3II and P62 in BEAS-2B cells. (c) Autophagosomes and autolysosomes were observed and counted under a transmission electron microscope. (The red arrow indicates mitochondria, the blue arrow indicates rough endoplasmic reticulum, the green arrow indicates Golgi apparatus, the pink arrow indicates autolysosomes and the yellow arrow indicates autophagosomes) (d) Comparison of the number of autophagosomes and autolysosomes. (e) Immunofluorescence analysis was used to detect the expression of LC3II and P62. (f) CCK-8 assays were used to determine the nature of autophagy in BEAS-2B cells after treatment with LPS for 6 h. (n=3-4) \*P < 0.05, \*\*P < 0.01, \*\*\*P < 0.001, \*\*\*\*P < 0.0001.

Immunofluorescence staining (Figure 3e) showed that the expression of LC3 was increased in LPS-induced cells but decreased by treatment with CAP. Finally, the characteristics of autophagy in BEAS-2B cells after 6 h of LPS stimulation were determined by CCK-8 assays (Figure 3f) and MTS assays (Figure S2b). The results showed a more pronounced decrease in cell viability in response to the combination of LPS and the autophagy agonist Rapa. On the other hand, cell viability was partially restored in the LPS+3-MA and LPS+Baf-A1 groups. These results indicated that cell viability was significantly decreased after 6 h of LPS stimulation, suggesting that the autophagy observed at this time point has a damaging effect. However, CAP protected cells from LPS-induced damage.<sup>46</sup> Therefore, CAP protects against LPS-induced autophagic death.

## CAP Regulates LPS-Induced Inflammation and Autophagy Through the TRPV1/AKT Axis

To explore the relationship between CAP and the TRPV1/AKT axis and its regulation of inflammation and autophagy, BEAS-2B cells were pretreated with the TRPV1 inhibitor AMG9810 or the AKT activator SC79 before CAP treatment. WB revealed (Figure 4a and b) that LPS upregulated p-AKT and LC3 protein expression while downregulating P62 expression (Figure 4c and d). However, pretreatment with CAP reversed these LPS-induced changes. However, the effect of CAP was attenuated when TRPV1 was inhibited or AKT was further activated. Immunofluorescence staining showed an increase in the expression of LC3 in cells induced by LPS. However, this upregulation was attenuated after treatment with CAP. Interestingly, the therapeutic effect of CAP was reversed after the addition of AMG9810 or SC79, resulting in a decrease in the expression of LC3, while the expression of P62 showed the opposite changes (Figure 4e). These findings suggested that CAP could modulate LPS-induced autophagy through the TRPV1/AKT axis. Furthermore, the ELISA (Figure 4f) and qRT-PCR (Figure 4g) results demonstrated that CAP pretreatment reversed the increase in inflammatory factors and inflammatory genes induced by LPS. However, inhibiting TRPV1 or further activating AKT weakened this effect. These results further suggest that CAP can regulate LPS-induced inflammation through the TRPV1/AKT axis. Finally, the assessment of cell viability (Figure 4h and Figure S2c) showed that CAP pretreatment reversed the decrease in cell viability caused by LPS, while the addition of AMG9810 and SC79 abrogated this effect. These results provide additional evidence that CAP can modulate the LPS-induced decrease in BEAS-2B cell viability through the TRPV1/AKT axis. To summarize, this preliminary evidence suggests that the therapeutic effect of CAP on the LPS-induced ALI model in BEAS-2B cells is mediated by the TRPV1/AKT axis.

## CAP Alleviates LPS-Induced ALI in Mice

We used HE staining and IHC to assess the protective effects of CAP on lung tissue in a mouse model of ALI. Histological examination of lung tissues (Figure 5a and b) in the Vehicle and CAP groups revealed normal lung structures. In contrast, the lung tissues of LPS-stimulated mice in the model group exhibited significant histopathological alterations, including hyperemia, hemorrhage, edema of the alveolar wall, and inflammatory cell infiltration. However, treatment with 8 mg/kg CAP ameliorated these pathological changes. Immunohistochemical analysis (Figure 5c and d) demonstrated that the expression of TNF- $\alpha$ , P-AKT, and LC3 was reduced in the control group, and these levels increased after LPS administration. However, CAP treatment reversed the LPS-induced increase in these markers. Moreover, the expression of TRPV1 was increased in the CAP and treatment groups, and it was reduced in the normal and LPS groups. Thus, CAP alone did not cause any harm to mouse lung tissue, while pretreatment with CAP reversed LPS-induced ALI in mice. These findings suggested that CAP effectively reduced the expression of TNF- $\alpha$ , P-AKT, and LC3 in ALI, and this effect was likely achieved through the modulation of the TRPV1/AKT axis, which was consistent with the in vitro results.

## CAP Inhibits the Secretion of Inflammatory Cytokines and the Expression of Inflammation-Related Genes in Mice with ALI

Total BALF protein levels (Figure 6a) and the lung dry-to-wet weight ratio (Figure 6b) were significantly elevated in the LPS-treated group compared to the control group. However, treatment with CAP effectively reversed these abnormalities. The levels of inflammatory mediators in the serum of mice were assessed by ELISA, and the expression levels of inflammatory genes in mouse lung tissues were determined by qRT-PCR. Notably, CAP treatment significantly reduced LPS-induced TNF- $\alpha$ , IL-6, and IL-1 $\beta$  secretion (Figure 6c) and expression (Figure 6d). These findings suggested that CAP mitigates LPS-induced inflammation by

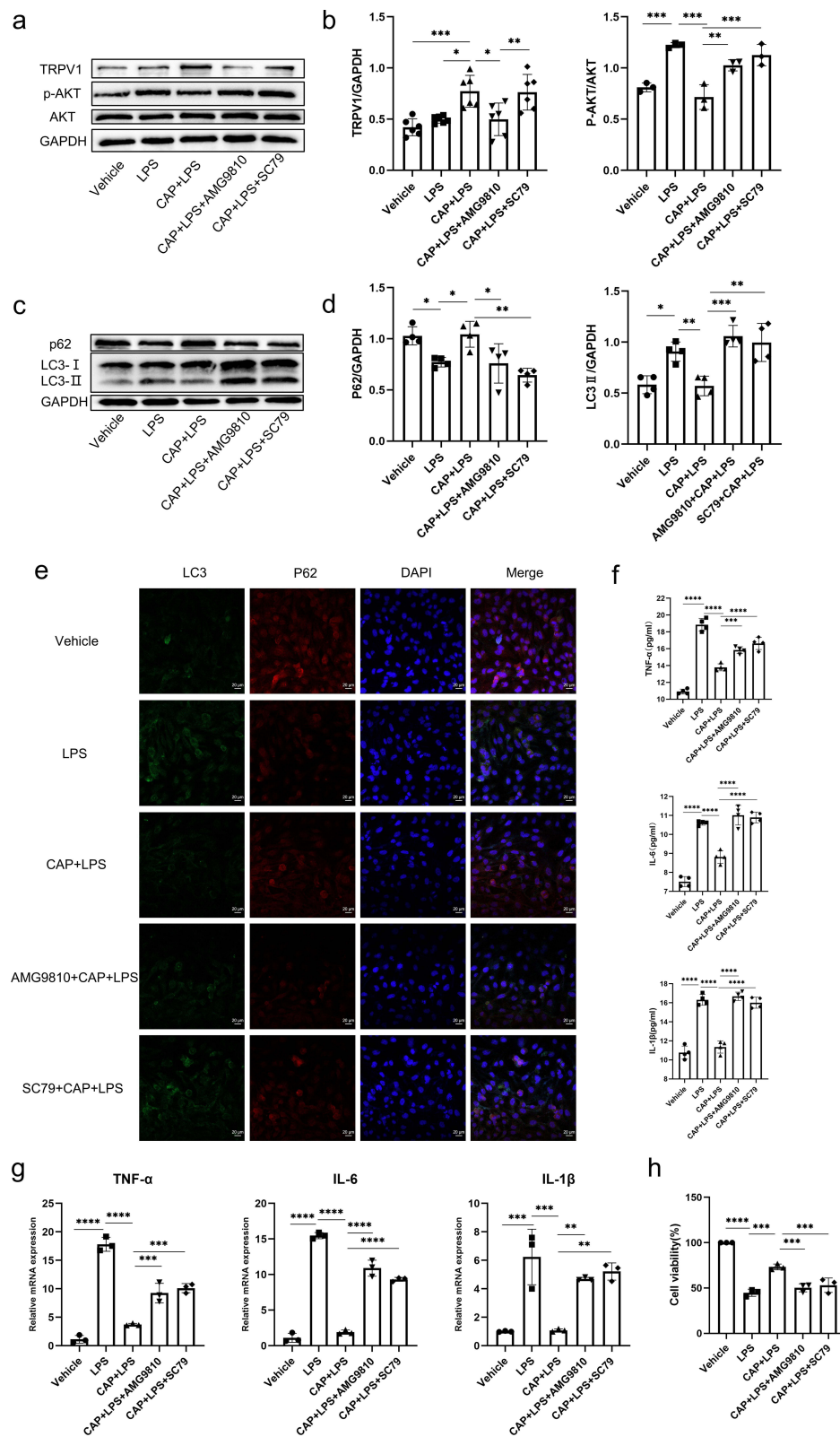


**Figure 4** CAP regulates injurious autophagy and inflammation through the TRPV1/AKT axis. (a) The expression levels of critical proteins involved in the TRPV1/AKT axis were measured by WB. (b) Statistical analysis of TRPV1 and p-AKT in BEAS-2B cells. (c) The expression levels of autophagy-related proteins were measured by WB. (d) Statistical analysis of LC3II and P62 in BEAS-2B cells. (e) Immunofluorescence analysis was used to detect the expression of LC3II and P62. (f) ELISA kits were used to analyze the changes in the inflammatory factors TNF- $\alpha$ , IL-6, and IL-1 $\beta$ . (g) qRT-PCR was used to analyze the changes in the inflammatory genes TNF- $\alpha$ , IL-6, and IL-1 $\beta$ . (h) Cell viability was assessed using the CCK-8 assay. (n=3~6) \*P < 0.05, \*\*P < 0.01, \*\*\*P < 0.001, \*\*\*\*P < 0.0001.

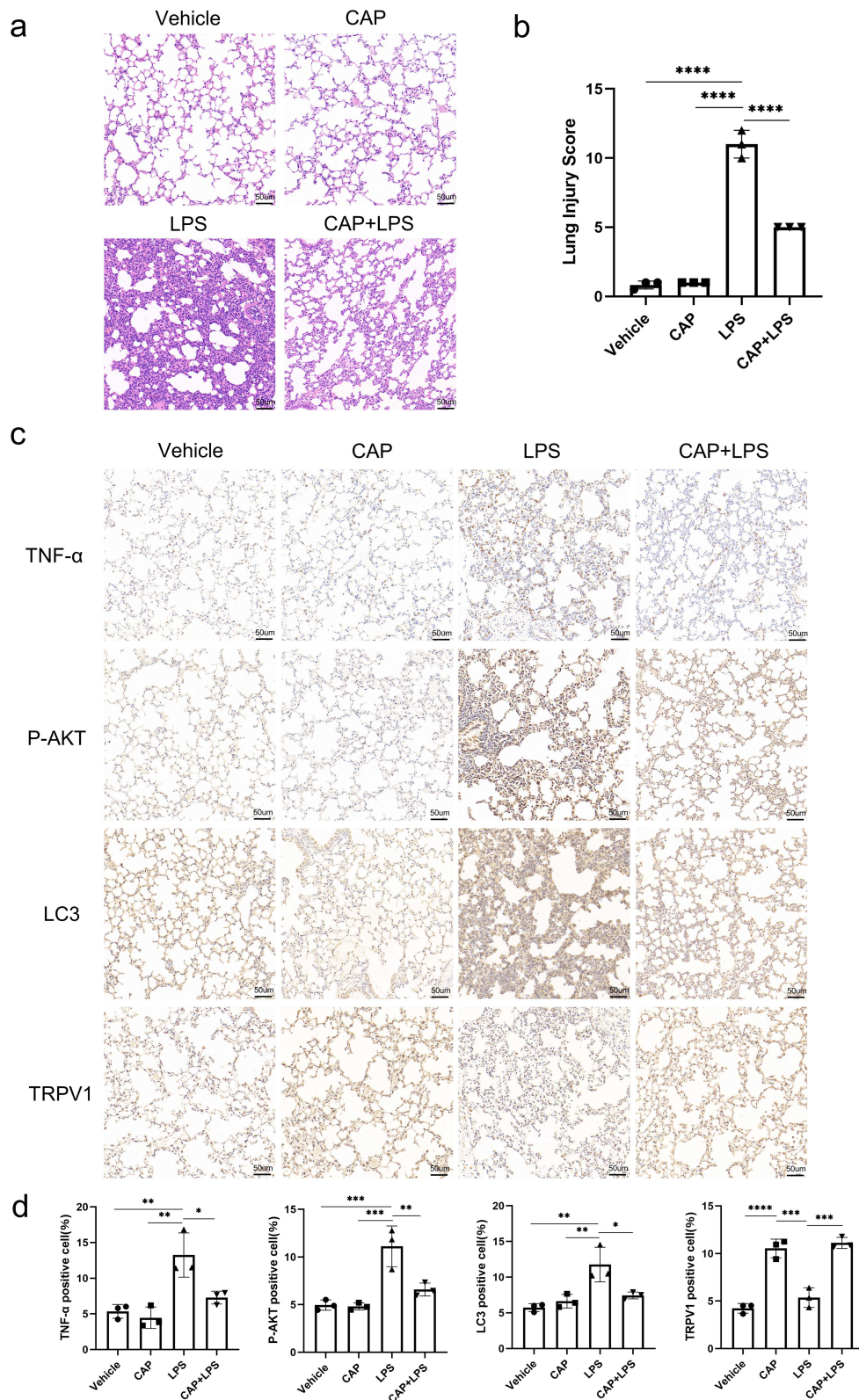


**Figure 5** Effect of LPS on lung tissues, as shown by HE staining and immunohistochemical analysis (n=3). (a) Representative HE-stained image of mouse lung tissue (50 μm). (b) Statistical analysis of HE staining. (c) Immunohistochemical section scanning (50 μm). (d) Statistical analysis of the IHC results. (n=3) \*P < 0.05, \*\*P < 0.01, \*\*\*P < 0.001, \*\*\*\*P < 0.0001.

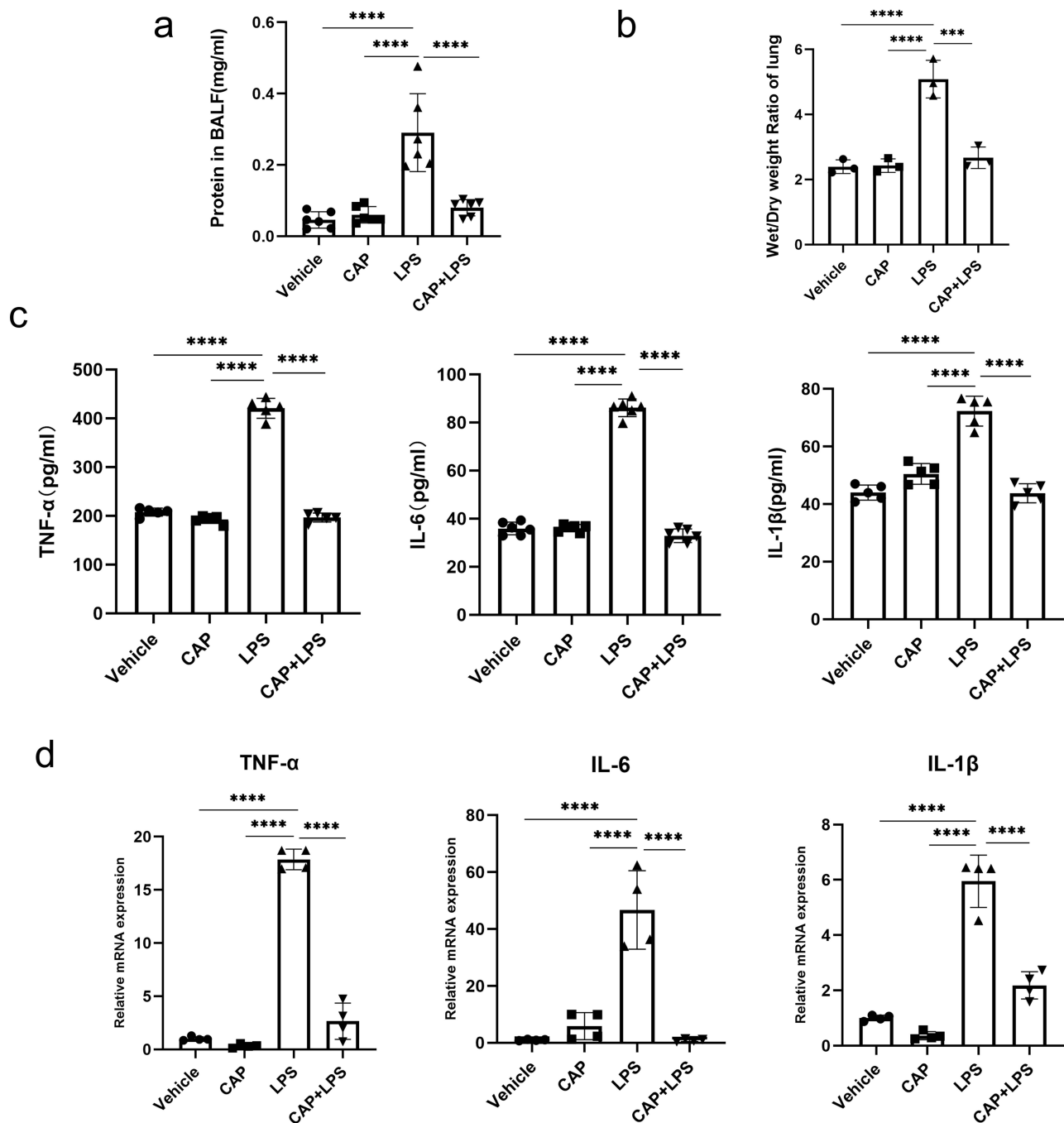


**Figure 6** CAP can alleviate inflammation in mice with LPS-induced ALI. (a) The total protein concentrations in mouse BALF were measured using a BCA assay kit. (b) The lung dry/wet weight ratios of mice. (c) ELISA was used to measure the levels of the inflammatory factors TNF- $\alpha$ , IL-6, and IL-1 $\beta$  in mouse serum. (d) qRT-PCR was used to determine the expression levels of the inflammatory genes TNF- $\alpha$ , IL-6, and IL-1 $\beta$  in the lung tissue in each group of mice. (n=3~6) \*\*\*P < 0.001, \*\*\*\*P < 0.0001.

inhibiting the recruitment of inflammatory cells, decreasing the secretion of proinflammatory cytokines, and reducing the expression of inflammation-related genes.

## Schematic Study Diagram

The molecular mechanism of CAP in the treatment of LPS-induced ALI is shown in Figure 7. CAP can specifically activate TRPV1 to reduce the expression of LC3, upregulate the expression of P62 indicating the inhibition of autophagy,

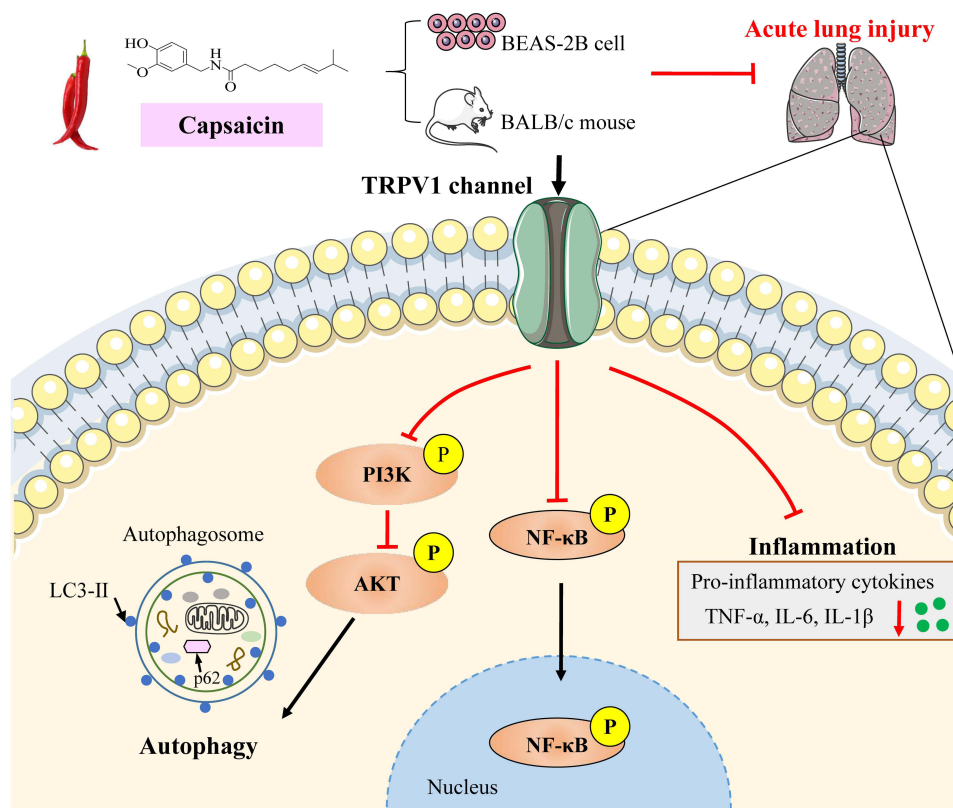


**Figure 7** Graphical illustration of CAP preconditioning inhibition of LPS-induced inflammation and autophagy through the TRPV1/AKT pathway.

and reduce the release of the inflammatory cytokines TNF- $\alpha$ , IL-6, and IL-1 $\beta$  through the suppression of the PI3K/AKT signaling pathway.

## Discussion

ALI is an inflammatory disease with a poor prognosis that is difficult to treat.<sup>47</sup> Imbalanced inflammatory responses exacerbate injury to endothelial or epithelial cells,<sup>48,49</sup> leading to an increase in lung surfactant protein levels.<sup>50</sup> Histologically, ALI is characterized by pulmonary fibrosis, heightened alveolar-capillary permeability, extensive apoptosis of alveolar epithelial cells, and a pronounced acute inflammatory response.<sup>51</sup> Although significant progress has been made in biomedical research, breakthroughs in the treatment of ALI are still limited.

CAP is a naturally occurring plant chemical with important applications in various drug formulations, as demonstrated by various experimental and clinical applications.<sup>52</sup> In certain aspects of inflammation, research studies have indicated that CAP can confer protection to mice against acute liver injury through the downregulation of proinflammatory cytokine expression.<sup>53,54</sup> CAP can also inhibit the calcification of aortic valve interstitial cells through the NF- $\kappa$ B/AKT/ERK1/2 pathway, which is sensitive to oxidative stress and inflammation.<sup>55</sup> Markers of the AKT, ERK1/2, and NF- $\kappa$ B signaling pathways, including phosphorylated AKT, ERK1/2, NF- $\kappa$ B, and I $\kappa$ B $\alpha$ , was upregulated in calcified cells, and they are significantly downregulated after CAP treatment. Moreover, a 2023 study indicated that the traditional Chinese medicine salidroside can protect against PM2.5-induced lung injury by inhibiting cell pyroptosis and apoptosis through the NF- $\kappa$ B pathway.<sup>56</sup> These findings further confirm the comprehensive and overall protective effect of traditional Chinese medicine on lung injury. Therefore, based on previous research and our current results, we believe that CAP may have a certain therapeutic effect on inflammatory lung diseases by modulating the NF- $\kappa$ B and Pi3k/AKT pathways. Moreover, our RNA sequencing results indicated that CAP, a drug with extremely low toxicity, may have a preventive effect on ALI at the overall level through different targets and potential signaling pathways. Our research

team will continue to verify other pathways identified via RNA sequencing, such as the JAK/STAT pathway, in subsequent experiments to provide a more comprehensive experimental basis for the clinical application of CAP.

Autophagy is a major intracellular degradation system, that is a multistep biological process. In ALI caused by multiple inducers, autophagy activation is present in various injured cells.<sup>57,58</sup> However, the functional role of autophagy is still controversial.

To date, there have been relatively few reports on inflammation, autophagy and CAP specifically targeting TRPV1 and ALI in BEAS-2B cell models. In addition, few studies have been conducted on the relationship between TRPV1 and the AKT axis, and we chose to explore the correlation and mechanism between them. In this study, we established an ALI model using LPS in BEAS-2B and BALB/c mice, RNA sequencing and *in vivo* and *in vitro* experiments were used to explore the therapeutic effect of CAP on ALI in terms of inflammation and autophagy.

First, we used RNA sequencing to screen potential targets and signaling pathways by which CAP can treat ALI. Based on the KEGG and GO analysis results, we selected the PI3K/AKT and NF- $\kappa$ B pathways, which are both related to inflammation, for validation. PI3K/AKT and NF- $\kappa$ B both play important roles in ALI. Previous studies have shown that the expression of phosphorylated PI3K, AKT, and NF- $\kappa$ B is upregulated in LPS-induced ALI, and the upregulation of phosphorylation markers is ameliorated after drug treatment.<sup>59,60</sup> In our study, we observed that pretreatment with CAP effectively mitigated lung injury induced by LPS, as evidenced by reductions in pulmonary edema and inflammatory cell infiltration. Furthermore, increased levels of proinflammatory cytokines, such as TNF- $\alpha$ , IL-6, and IL-1 $\beta$ , are often associated with a poor prognosis in ALI patients. In this study, we demonstrated that CAP treatment inhibited the expression of TNF- $\alpha$ , IL-6, and IL-1 $\beta$  in models of LPS-induced ALI *in vivo* and *in vitro*, suggesting its protective role in ameliorating inflammation.

Moreover, we confirmed that autophagy activated by LPS stimulation of human normal lung epithelial BEAS-2B cells for 6 h induced damage, as evidenced by the increased number of autophagosomes and autolysosomes observed by TEM, the upregulation of the protein expression and colocalization of the autophagy marker LC3, and the down-regulation of P62. The immunohistochemical results showed an increase in LC3 and inflammation levels in the lung tissue of LPS-induced mice, which were decreased in the treatment group. We further determined that LPS-induced autophagy mediated death after pretreatment with Rapa, 3-MA, or Baf-A1. These results indicate the activation of autophagic death in the development of ALI, which could be reversed by CAP.

The relationship between TRPV1 and the AKT axis in the ALI model of BEAS-2B cells remains unclear. Therefore, we used the TRPV1 inhibitor AMG9810 and the AKT activator SC79 to treat BEAS-2B cells before CAP treatment. WB, ELISA, and qRT-PCR showed that CAP pretreatment could partially reverse LPS-induced inflammation and excessive autophagy. Subsequently, the addition of AMG9810 and SC79 abrogated the therapeutic effect of CAP. Moreover, *in vivo* experiments demonstrated that CAP had the same inhibitory effects on inflammation and injurious autophagy in LPS-induced ALI mice, thereby reducing the damage caused by ALI. This finding suggests that the therapeutic effect of CAP on LPS-induced inflammation and autophagy is mediated by the TRPV1/AKT axis. Therefore, this study provides an experimental basis for the clinical use of CAP in the treatment of ALI.

## Conclusion

In summary, we demonstrated that CAP could reduce autophagic death and attenuate inflammatory responses by regulating the TRPV1/AKT signaling pathway, thereby attenuating LPS-induced ALI *in vitro* and *in vivo*. These findings establish a basis for future clinical investigations into the underlying pathological mechanisms and potential intervention strategies for the treatment of lung injury.

## Abbreviations

CAP, capsaicin; LPS, lipopolysaccharide; ALI, acute lung injury; BEAS-2B, bronchial epithelial cells transformed with Ad12-SV40 2B; TRPV1, transient receptor potential vanilloid type 1; WB, Western blotting; qRT-PCR, quantitative real-time reverse transcription PCR; ELISA, enzyme-linked immunosorbent assay; TEM, transmission electron microscopy; TNF- $\alpha$ , tumor necrosis factor- $\alpha$ ; IL-6, interleukin-6; IL-1 $\beta$ , interleukin-1 $\beta$ ; ARDS, acute respiratory distress syndrome; DMEM, Dulbecco's

modified Eagle's medium; PBS, phosphate-buffered saline; PMSF, phenylmethanesulfonyl fluoride; BCA, the bicinchoninic acid; BSA, bovine serum albumin; Rapa, Rapamycin; 3-MA, 3-methyladenine; Baf-A1, bafilomycin A1; TBST, Tris-buffered saline containing Tween-20; ECL, chemiluminescence; IHC, Immunohistochemistry.

## Data Sharing Statement

The data that support the findings of this study are available from the corresponding author upon reasonable request.

## Ethical Approval and Consent to Participate

All experiments in the present study were conformed to the Guide for the Care and Use of Laboratory Regulations and were approved by the Institutional Experiment Committee of Sichuan Provincial People's Hospital (Number 326, 2023 of Sichuan Province People's Hospital).

## Acknowledgments

We wish to acknowledge all authors for their contributions to this article.

## Author Contributions

All authors made a significant contribution to the work reported, whether that is in the conception, study design, execution, acquisition of data, analysis and interpretation, or in all these areas; took part in drafting, revising or critically reviewing the article; gave final approval of the version to be published; have agreed on the journal to which the article has been submitted; and agree to be accountable for all aspects of the work.

## Funding

This work was supported by grants from the National Natural Science Foundation of China (81871611, 82303712), the Foundation of Sichuan Provincial Science and Technology (2022YFS0602), Hainan Province Science and Technology Special Fund (ZDKJ202004, ZDKJ2021038), the Foundation of Sichuan Provincial People's Hospital (2022QN43) and China Postdoctoral Science Foundation (2023M740520).

## Disclosure

The author reports no conflicts of interest in this work.

## References

1. Matthay MA, Ware LB, Zimmerman GA. The acute respiratory distress syndrome. *J Clin Invest*. 2012;122(8):2731–2740. doi:10.1172/JCI60331
2. Ranieri VM, Rubenfeld GD, Thompson BT, et al. Acute respiratory distress syndrome: the Berlin Definition. *JAMA*. 2012;307(23):2526–2533. doi:10.1001/jama.2012.5669
3. Ware LB, Matthay MA. The acute respiratory distress syndrome. *N Engl J Med*. 2000;342(18):1334–1349. doi:10.1056/NEJM200005043421806
4. Shi J, Zhao Y, Wang Y, et al. Inflammatory caspases are innate immune receptors for intracellular LPS. *Nature*. 2014;514(7521):187–192. doi:10.1038/nature13683
5. Wu Z, Wang Y, Lu S, Yin L, Dai L. SIRT3 alleviates sepsis-induced acute lung injury by inhibiting pyroptosis via regulating the deacetylation of FoxO3a. *Pulm Pharmacol Ther*. 2023;82:102244. doi:10.1016/j.pupt.2023.102244
6. Li M, Wang C, Xu WT, Zhong X. Sodium houttuynonate plays a protective role in the asthmatic airway by alleviating the NLRP3-related pyroptosis and Th1/Th2 immune imbalance. *Mol Immunol*. 2023;160:103–111. doi:10.1016/j.molimm.2023.06.013
7. Song H, Jiang L, Yang W, et al. Cryptotanshinone alleviates lipopolysaccharide and cigarette smoke-induced chronic obstructive pulmonary disease in mice via the Keap1/Nrf2 axis. *Biomed Pharmacother*. 2023;165:115105. doi:10.1016/j.biopha.2023.115105
8. Liu L, Zhang Y, Wang L, et al. Scutellarein alleviates chronic obstructive pulmonary disease through inhibition of ferroptosis by chelating iron and interacting with arachidonate 15-lipoxygenase. *Phytother Res*. 2023;2:4.
9. Chapa-Oliver AM, Mejia-Teniente L. Capsaicin: from plants to a cancer-suppressing agent. *Molecules*. 2016;21(8):931. doi:10.3390/molecules21080931
10. Li Q, Chang M, Lai R, et al. Potential benefits of spicy food consumption on cardiovascular outcomes in patients with diabetes: a cohort study of the China Kadoorie Biobank. *Nutrition*. 2023;112:112062. doi:10.1016/j.nut.2023.112062
11. Blair HA. Capsaicin 8% dermal patch: a review in peripheral neuropathic pain. *Drugs*. 2018;78(14):1489–1500. doi:10.1007/s40265-018-0982-7
12. Ghorbanpour A, Salari S, Baluchnejadmojarad T, Roghani M. Capsaicin protects against septic acute liver injury by attenuation of apoptosis and mitochondrial dysfunction. *Heliyon*. 2023;9(3):e14205. doi:10.1016/j.heliyon.2023.e14205

13. Lian YZ, Chang CC, Chen YS, Tinkov AA, Skalny AV, Chao JC. Lycium barbarum polysaccharides and capsaicin modulate inflammatory cytokines and colonic microbiota in colitis rats induced by dextran sulfate sodium. *J Clin Biochem Nutr.* 2022;71(3):229–237. doi:10.3164/jcbsn.21-174
14. Zheng Y, Chen J, Wu X, et al. Enhanced anti-inflammatory effects of silibinin and capsaicin combination in lipopolysaccharide-induced RAW264.7 cells by inhibiting NF- $\kappa$ B and MAPK activation. *Front Chem.* 2022;10:934541. doi:10.3389/fchem.2022.934541
15. Howard LR, Talcott ST, Brenes CH, Villalon B. Changes in phytochemical and antioxidant activity of selected pepper cultivars (*Capsicum* species) as influenced by maturity. *J Agric Food Chem.* 2000;48(5):1713–1720. doi:10.1021/jf990916t
16. Khan FA, Mahmood T, Ali M, Saeed A, Maalik A. Pharmacological importance of an ethnobotanical plant: *Capsicum annuum* L. *Nat Prod Res.* 2014;28(16):1267–1274. doi:10.1080/14786419.2014.895723
17. Maji AK, Banerji P. Phytochemistry and gastrointestinal benefits of the medicinal spice, *Capsicum annuum* L. (Chilli): a review. *J Complement Integr Med.* 2016;13(2):97–122. doi:10.1515/jcim-2015-0037
18. Chen H, Li N, Zhan X, et al. Capsaicin protects against lipopolysaccharide-induced acute lung injury through the HMGB1/NF- $\kappa$ B and PI3K/AKT/mTOR pathways. *J Inflamm Res.* 2021;14:5291–5304. doi:10.2147/JIR.S309457
19. Srinivasan K. Biological activities of red pepper (*Capsicum annuum*) and its pungent principle capsaicin: a review. *Crit Rev Food Sci Nutr.* 2016;56(9):1488–1500. doi:10.1080/10408398.2013.772090
20. Zhang S, Tang C, Wang X. Octreotide activates autophagy to alleviate lipopolysaccharide-induced human pulmonary epithelial cell injury by inhibiting the protein kinase B (AKT)/mammalian target of rapamycin (mTOR) signaling pathway. *Bioengineered.* 2022;13(1):217–226. doi:10.1080/21655979.2021.2012908
21. Meng Y, Pan M, Zheng B, et al. Autophagy attenuates angiotensin II-induced pulmonary fibrosis by inhibiting redox imbalance-mediated NOD-like receptor family pyrin domain containing 3 inflammasome activation. *Antioxid Redox Signal.* 2019;30(4):520–541. doi:10.1089/ars.2017.7261
22. Li Y, Yu G, Yuan S, et al. Cigarette smoke-induced pulmonary inflammation and autophagy are attenuated in Ephx2-deficient mice. *Inflammation.* 2017;40(2):497–510. doi:10.1007/s10753-016-0495-z
23. Chu R, Wang J, Bi Y, Nan G. The kinetics of autophagy in the lung following acute spinal cord injury in rats. *Spine J.* 2018;18(5):845–856. doi:10.1016/j.spinee.2018.01.001
24. Chang AL, Ulrich A, Suliman HB, Piantadosi CA. Redox regulation of mitophagy in the lung during murine *Staphylococcus aureus* sepsis. *Free Radic Biol Med.* 2015;78:179–189. doi:10.1016/j.freeradbiomed.2014.10.582
25. Guo L, Wu X, Zhao S, Zhang X, Qian G, Li S. Autophagy inhibition protects from alveolar barrier dysfunction in LPS-induced ALI mice by targeting alveolar epithelial cells. *Respir Physiol Neurobiol.* 2021;283:103532. doi:10.1016/j.resp.2020.103532
26. Huang S, Xue Y, Chen W, et al. Fibroblast growth factor 10 alleviates acute lung injury by inhibiting excessive autophagy via Nrf2. *J Endocrinol.* 2023;259(1). doi:10.1530/JOE-23-0095
27. Sun Q, Zhang H, Du HB, et al. Estrogen Alleviates Posthemorrhagic Shock Mesenteric Lymph-Mediated Lung Injury Through Autophagy Inhibition. *Shock.* 2023;59(5):754–762. doi:10.1097/SHK.0000000000002102
28. Sun Y, Li C, Shu Y, et al. Inhibition of autophagy ameliorates acute lung injury caused by avian influenza A H5N1 infection. *Sci Signal.* 2012;5(212):ra16. doi:10.1126/scisignal.2001931
29. Hu R, Chen ZF, Yan J, et al. Complement C5a exacerbates acute lung injury induced through autophagy-mediated alveolar macrophage apoptosis. *Cell Death Dis.* 2014;5(7):e1330–e1330. doi:10.1038/cddis.2014.274
30. Zhu Q, Wang H, Wang H, et al. Protective effects of ethyl pyruvate on lipopolysaccharide-induced acute lung injury through inhibition of autophagy in neutrophils. *Mol Med Rep.* 2017;15(3):1272–1278. doi:10.3892/mmr.2017.6118
31. Qian F, He S, Yang X, Chen X, Zhao S, Wang J. Circular RNA DHTKD1 targets miR-338-3p/ETS1 axis to regulate the inflammatory response in human bronchial epithelial cells. *Exp Ther Med.* 2023;26(1):316. doi:10.3892/etm.2023.12015
32. Miao RF, Tu J. LncRNA CDKN2B-AS1 interacts with LIN28B to exacerbate sepsis-induced acute lung injury by inducing HIF-1 $\alpha$ /NLRP3-mediated pyroptosis. *Kaohsiung J Med Sci.* 2023;39(9):883–895. doi:10.1002/kjm2.12697
33. Bouyer PG, Tang X, Weber CR, Shen L, Turner JR, Matthews JB. Capsaicin induces NKCC1 internalization and inhibits chloride secretion in colonic epithelial cells independently of TRPV1. *Am J Physiol Gastrointest Liver Physiol.* 2013;304(2):G142–156. doi:10.1152/ajpgi.00483.2011
34. Jiao Y, Shen F, Wang Z, et al. Genipin, a natural AKT inhibitor, targets the PH domain to affect downstream signaling and alleviates inflammation. *Biochem Pharmacol.* 2019;170:113660. doi:10.1016/j.bcp.2019.113660
35. Liu T, Wu B, Wang Y, et al. Particulate matter 2.5 induces autophagy via inhibition of the phosphatidylinositol 3-kinase/Akt/mammalian target of rapamycin kinase signaling pathway in human bronchial epithelial cells. *Mol Med Rep.* 2015;12(2):1914–1922. doi:10.3892/mmr.2015.3577
36. Wang X, Liu F, Xu M, Wu L. Penehyclidine hydrochloride alleviates lipopolysaccharide-induced acute respiratory distress syndrome in cells via regulating autophagy-related pathway. *Mol Med Rep.* 2021;23(2).
37. Yang N, Shang Y. Ferrostatin-1 and 3-methyladenine ameliorate ferroptosis in OVA-induced asthma model and in IL-13-challenged BEAS-2B cells. *Oxid Med Cell Longev.* 2022;2022:9657933. doi:10.1155/2022/9657933
38. Zhang Y, Yang S, Qiu Z, et al. Pyrogallol enhances therapeutic effect of human umbilical cord mesenchymal stem cells against LPS-mediated inflammation and lung injury via activation of Nrf2/HO-1 signaling. *Free Radic Biol Med.* 2022;191:66–81. doi:10.1016/j.freeradbiomed.2022.08.030
39. Xu L, Li X, Wang H, Xie F, Liu H, Xie J. Cigarette smoke triggers inflammation mediated by autophagy in BEAS-2B cells. *Ecotoxicol Environ Saf.* 2019;184:109617. doi:10.1016/j.ecoenv.2019.109617
40. Liu P, Hao J, Zhao J, et al. Integrated network pharmacology and experimental validation approach to investigate the therapeutic effects of capsaicin on lipopolysaccharide-induced acute lung injury. *Mediators Inflamm.* 2022;2022:9272896. doi:10.1155/2022/9272896
41. Cabral LD, Giusti-Paiva A. The transient receptor potential vanilloid 1 antagonist capsazepine improves the impaired lung mechanics during endotoxemia. *Basic Clin Pharmacol Toxicol.* 2016;119(5):421–427. doi:10.1111/bcpt.12605
42. Joffre J, Wong E, Lawton S, et al. N-Oleoyl dopamine induces IL-10 via central nervous system TRPV1 and improves endotoxemia and sepsis outcomes. *J Neuroinflammation.* 2022;19(1):118. doi:10.1186/s12974-022-02485-z
43. Meng L, Li L, Lu S, et al. The protective effect of dexmedetomidine on LPS-induced acute lung injury through the HMGB1-mediated TLR4/NF- $\kappa$ B and PI3K/Akt/mTOR pathways. *Mol Immunol.* 2018;94:7–17. doi:10.1016/j.molimm.2017.12.008

44. Li T, Wu YN, Wang H, Ma JY, Zhai SS, Duan J. Dapk1 improves inflammation, oxidative stress and autophagy in LPS-induced acute lung injury via p38MAPK/NF- $\kappa$ B signaling pathway. *Mol Immunol*. 2020;120:13–22. doi:10.1016/j.molimm.2020.01.014
45. Slavina SA, Leonard A, Grose V, Fazal F, Rahman A. Autophagy inhibitor 3-methyladenine protects against endothelial cell barrier dysfunction in acute lung injury. *Am J Physiol Lung Cell Mol Physiol*. 2018;314(3):L388–L396. doi:10.1152/ajplung.00555.2016
46. Kong L, Deng J, Zhou X, et al. Sitagliptin activates the p62-Keap1-Nrf2 signalling pathway to alleviate oxidative stress and excessive autophagy in severe acute pancreatitis-related acute lung injury. *Cell Death Dis*. 2021;12(10):928. doi:10.1038/s41419-021-04227-0
47. Fanelli V, Ranieri VM. Mechanisms and clinical consequences of acute lung injury. *Ann Am Thorac Soc*. 2015;12(Suppl 1):S3–8. doi:10.1513/AnnalsATS.201407-340MG
48. Seki H, Tasaka S, Fukunaga K, et al. Effect of Toll-like receptor 4 inhibitor on LPS-induced lung injury. *Inflamm Res*. 2010;59(10):837–845. doi:10.1007/s00011-010-0195-3
49. Patel BV, Wilson MR, O’Dea KP, Takata M. TNF-induced death signaling triggers alveolar epithelial dysfunction in acute lung injury. *J Immunol*. 2013;190(8):4274–4282. doi:10.4049/jimmunol.1202437
50. Pierrakos C, Karanikolas M, Scolletta S, Karamouzos V, Velissaris D. Acute respiratory distress syndrome: pathophysiology and therapeutic options. *J Clin Med Res*. 2012;4(1):7–16. doi:10.4021/jocmr761w
51. Ward PA, Grailer JJ. Acute lung injury and the role of histones. *Transl Respir Med*. 2014;2(1):1. doi:10.1186/2213-0802-2-1
52. Alonso-Villegas R, González-Amaro RM, Figueroa-Hernández CY, Rodríguez-Buenfil IM. The genus capsicum: a review of bioactive properties of its polyphenolic and capsaicinoid composition. *Molecules*. 2023;28(10):4239. doi:10.3390/molecules28104239
53. Fernandes ES, Cerqueira AR, Soares AG, Costa SK. Capsaicin and its role in chronic diseases. *Adv Exp Med Biol*. 2016;929:91–125. doi:10.1007/978-3-319-41342-6\_5
54. Zhan X, Zhang J, Chen H, et al. Capsaicin alleviates Acetaminophen-induced acute liver injury in mice. *Clin Immunol*. 2020;220:108578.
55. Adhikari R, Jung J, Shiwakoti S, et al. Capsaicin inhibits aortic valvular interstitial cell calcification via the redox-sensitive NF $\kappa$ B/AKT/ERK1/2 pathway. *Biochem Pharmacol*. 2023;212:115530. doi:10.1016/j.bcp.2023.115530
56. Shi S, Huang D, Wu Y, et al. Salidroside pretreatment alleviates PM(2.5) caused lung injury via inhibition of apoptosis and pyroptosis through regulating NLRP3 Inflammasome. *Food Chem Toxicol*. 2023;177:113858. doi:10.1016/j.ft.2023.113858
57. Mizushima N, Komatsu M. Autophagy: renovation of cells and tissues. *Cell*. 2011;147(4):728–741. doi:10.1016/j.cell.2011.10.026
58. Khandia R, Dadar M, Munjal A, et al. A comprehensive review of autophagy and its various roles in infectious, non-infectious, and lifestyle diseases: current knowledge and prospects for disease prevention, novel drug design, and therapy. *Cells*. 2019;8(7):674. doi:10.3390/cells8070674
59. Ma Y, Xu H, Chen G, et al. Uncovering the active constituents and mechanisms of Rujin Jiedu powder for ameliorating LPS-induced acute lung injury using network pharmacology and experimental investigations. *Front Pharmacol*. 2023;14:1186699. doi:10.3389/fphar.2023.1186699
60. Wang L, Jiang S, Li X, Lin T, Qin T. Astringin protects LPS-induced toxicity by suppressing oxidative stress and inflammation via suppression of PI3K/AKT/NF- $\kappa$ B pathway for pediatric acute lung injury. *Naunyn Schmiedebergs Arch Pharmacol*. 2023;396(10):2369–2377. doi:10.1007/s00210-023-02439-z

## Publish your work in this journal

The Journal of Inflammation Research is an international, peer-reviewed open-access journal that welcomes laboratory and clinical findings on the molecular basis, cell biology and pharmacology of inflammation including original research, reviews, symposium reports, hypothesis formation and commentaries on: acute/chronic inflammation; mediators of inflammation; cellular processes; molecular mechanisms; pharmacology and novel anti-inflammatory drugs; clinical conditions involving inflammation. The manuscript management system is completely online and includes a very quick and fair peer-review system. Visit <http://www.dovepress.com/testimonials.php> to read real quotes from published authors.

Submit your manuscript here: <https://www.dovepress.com/journal-of-inflammation-research-journal>